Force Perception in Robot-Assisted Surgery: Integrating Force Sensing, Haptic Feedback, and AI-Based Estimation for Next-Generation Surgical Robotics

Timothy Ayelagbe
Dept. of Electronic and Electrical Engineering
Obafemi Awolowo University
Ile-Ife, Nigeria
timothyayelagbe@gmail.com

Promise Osunyemi
Dept. of Electronic and Electrical Engineering
Obafemi Awolowo University
Ile-Ife, Nigeria
promiseosunyemi04@gmail.com

Glory Akanbi
Dept. of Electronic and Electrical Engineering
Obafemi Awolowo University
Ile-Ife, Nigeria
gloryinioluwa1@gmail.com

***Abstract*—Robot-assisted surgery (RAS) has transformed minimally invasive procedures by delivering enhanced dexterity, tremor filtration, and three-dimensional visualization. However, the near-complete absence of force feedback in most deployed platforms remains a critical limitation, compelling surgeons to infer tissue interaction forces from visual cues alone, a deficiency associated with elevated tissue trauma, excess grasping forces, and prolonged training curves. This paper presents an integrative review of three coupled technology domains—force sensing hardware, haptic feedback modalities, and artificial intelligence (AI)-based force estimation—evaluating strain gauges, piezoelectric transducers, fiber Bragg grating (FBG) sensors, and model-based observers for sensing; kinesthetic, vibrotactile, and pneumatic tactile modalities for feedback; and deep learning, physics-informed neural networks (PINNs), and Gaussian process regression for sensorless force estimation. Drawing on these analyses, a three-layer conceptual framework for next-generation force-aware surgical robots is proposed, with explicit consideration of deployment feasibility in resource-limited environments, including sub-Saharan African clinical contexts. The framework integrates FBG sensing, multimodal AI estimation, and multi-channel haptic rendering within a unified co-designed architecture, targeting an end-to-end feedback latency below 15 ms that an analytical pipeline budget indicates is achievable with margin. A Monte Carlo simulation of the proposed inverse-variance sensor fusion further shows a 73% reduction in root-mean-square error (RMSE) over either sensing channel alone, with graceful degradation rather than failure when one channel is impaired. Both results are numerical projections from literature-representative parameters rather than hardware measurements, reported alongside the review's broader conceptual contribution.**

***Index Terms*—robot-assisted surgery, force sensing, haptic feedback, fiber Bragg grating, deep learning, sensor fusion, Monte Carlo simulation, surgical robotics, physics-informed neural networks, minimally invasive surgery, LMIC deployment.**

I. INTRODUCTION

The integration of robotic platforms into minimally invasive surgery (MIS) represents one of the most consequential transitions in modern surgical practice. Systems such as the da Vinci Surgical System provide surgeons with wristed instrumentation, motion scaling, tremor filtration, and stereoscopic visualization, enabling procedures through 8–12 mm incisions that previously demanded open surgery [1]. Global utilization of robot-assisted surgery exceeded two million procedures annually as of recent reports, with adoption accelerating across high- and middle-income economies [2].

Despite these advances, a fundamental sensory deficit persists: haptic feedback is almost entirely absent. In conventional surgery, the operative hand continuously transmits tactile and kinesthetic information—tissue stiffness, texture, and structural proximity. Robotic teleoperation severs this mechanical chain. Surgeons must reconstruct tissue forces from visual cues alone: deformation patterns, instrument deflection, and suture tension [3]. The consequences are well-documented. Bergholz et al. [4] conducted a systematic review and meta-analysis demonstrating that haptic feedback significantly reduces forces applied by surgeons (Hedges' $g = 0.83$, 95% confidence interval (CI) 0.63–1.03, for average force reduction), with direct implications for tissue safety and anastomotic integrity.

The commercial landscape is beginning to respond. The da Vinci 5, U.S. Food and Drug Administration (FDA)-cleared in March 2024, incorporates a Force Feedback (FFB) capability at the end-effector. Preclinical evaluation by Awad et al. [5] demonstrated that FFB-equipped participants applied up to 43% less force on tissue during suturing tasks, with benefits across novice and experienced surgeons alike. However, current FFB implementation is limited to push-pull and compression forces; six-axis force/torque sensing and high-fidelity tactile rendering remain engineering challenges.

This paper delivers an integrative review of three enabling domains—force sensing hardware, haptic feedback modalities, and AI-driven force estimation—and proposes a conceptual framework for next-generation force-aware surgical robots. Unlike prior surveys of haptics [40] or vision-based force estimation [12] in isolation, this work treats sensing, estimation, and rendering as a single co-designed pipeline. Narrative reviews of Sub-Saharan African robotic-surgery feasibility [46] and surgical telementoring in low-resource settings [47] address infrastructure, training, and connectivity rather than intraoperative force perception; to our knowledge, this is among the first works to situate the force-sensing/haptics/AI integration problem specifically against that deployment context. Special emphasis is placed on deployment in low- and middle-income country (LMIC) contexts, including the Nigerian healthcare environment from which this work originates.

The contributions of this paper are: (1) an integrative review treating force sensing, haptic feedback, and AI-based force estimation as a single co-designed pipeline rather than separate technology tracks; (2) a three-layer conceptual framework with every non-standard design parameter explicitly flagged as an assumption pending hardware validation; (3) an analytical latency budget indicating the <15 ms target is achievable with margin; (4) a Monte Carlo simulation validating the proposed sensor-fusion mechanism under a simulated degradation event; and (5) a deployment analysis for LMIC and Sub-Saharan African contexts, including barriers specific to Nigeria.

II. Force Sensing Technologies

Integrating force sensing into surgical instruments imposes uniquely stringent constraints with no industrial parallel. Instrument shafts must accommodate sensing elements within outer diameters rarely exceeding 5–10 mm, while all patient-contact components must be biocompatible and endure repeated sterilization—typically autoclave conditions at 134°C—and must resist electromagnetic interference (EMI) from electrosurgical units. Clinically relevant tissue interaction forces span sub-Newton grasping delicacy to forces exceeding 15 N in dense tissue manipulation [8], [9].

A. Strain Gauge and Piezoresistive Sensors

Strain gauges represent the most mature force measurement technology. Mechanical deformation changes electrical resistance in a Wheatstone bridge configuration, yielding a compensated force signal. Puangmali et al. [13] demonstrated a triaxial distal force sensor measuring ±3 N axially and ±1.5 N radially with 0.02 N resolution. Practical limitations include wiring complexity through articulated wrist mechanisms, hysteresis reaching 3–5% of full scale, autoclave-induced calibration drift after 20–50 sterilization cycles, and inductive crosstalk from electrosurgical units exceeding 5% of full-scale output [9].

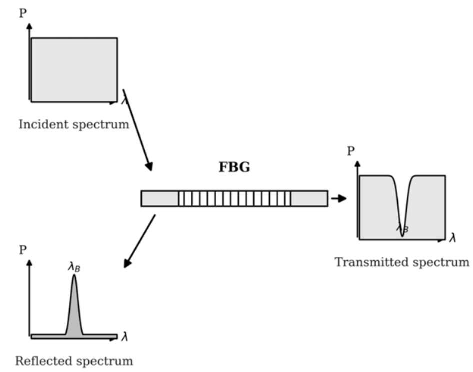

Fig. 1. Spectral filtering and strain-induced Bragg wavelength shift in a fiber Bragg grating: the FBG reflects a narrow spectral band at λ_B while transmitting the remainder (adapted from the standard FBG operating-principle illustration; cf. FBGS International [16]).

B. Piezoelectric Sensors

Piezoelectric transducers exploit spontaneous polarization of crystalline materials—lead zirconate titanate (PZT) and polyvinylidene fluoride (PVDF)—under mechanical stress. Their exceptional dynamic bandwidth (>100 kHz) and high sensitivity suit vibration-based tissue discrimination—detecting distinct signatures when cutting across fascial planes versus parenchymal tissue. The fundamental limitation is charge leakage: the mechanism cannot measure static or slowly varying forces, a significant constraint since surgical force dwell durations commonly exceed several seconds [14].

C. Fiber Bragg Grating Sensors

Fiber Bragg grating (FBG) sensors have emerged as the most promising technology for direct surgical force sensing. An FBG is a periodic refractive index modulation inscribed into single-mode optical fiber, as shown in Fig. 1. Applied strain shifts the Bragg wavelength according to:

$$\frac{\Delta\lambda_B}{\lambda_B} = (1 - p_e)\,\varepsilon + (\alpha_f + \xi)\,\Delta T \tag{1}$$

where $p_e \approx 0.22$ is the effective photoelastic coefficient, ε is longitudinal strain, $\alpha_f = 0.55 \times 10^{-6}\,{}^\circ\mathrm{C}^{-1}$ is fiber thermal expansion, and $\xi \approx 6.67 \times 10^{-6}\,{}^\circ\mathrm{C}^{-1}$ is the thermo-optic coefficient [15]. Multiple FBGs on a single fiber enable three-axis force and torque reconstruction. Key barriers include interrogator cost ($5,000–$40,000) and fiber fragility at articulated wrist joints, though femtosecond laser-inscribed FBGs retain >90% tensile strength [15].

D. Model-Based Estimation and Sensor Fusion

When direct tip sensing is infeasible, forces can be estimated using generalized momentum observers on the robot dynamics. The observer residual satisfies:

$$\dot{r}(t) = K_I \left[J^\top(\boldsymbol{\theta})\, F_{\text{ext}} - r(t) \right], \quad r(0) = 0 \tag{2}$$

where K_I is a positive definite observer gain, $J(\boldsymbol{\theta})$ is the configuration Jacobian, and F_{ext} is the external force vector [17]. Soft tissue interaction is modeled via Mooney–Rivlin

TABLE I
COMPARISON OF FORCE SENSING TECHNOLOGIES

Technology	**Res. (N)**	**Range (N)**	**EMI**	**Steril.**	**Limitation**
Strain Gauge	0.01–0.05	0–15	Low	Moderate	Wiring; hysteresis
Piezoelectric	High (dyn.)	Wide	Moderate	Good	No static sensing
FBG (optical)	0.03–0.1	0–20	Excellent	>50 cycles	Interrogator cost
MEMS Cap.	0.001–0.005	0–2	Low	Difficult	Fluid ingress
Model-Based	0.1–0.5	Model-dep.	Excellent	N/A (SW)	Model uncertainty

MEMS: micro-electro-mechanical systems. Sources: [8], [9], [13]

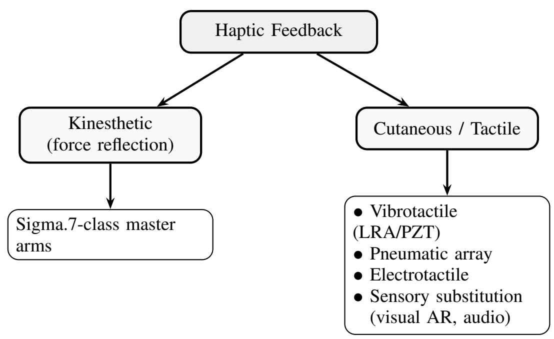

Fig. 2. Taxonomy of haptic feedback modalities surveyed in this section, organized by the two mechanistically distinct sensory channels they stimulate.

hyperelastic formulations: $W = C_{10}(I_1 - 3) + C_{01}(I_2 - 3)$, with constants identified from ex vivo mechanical testing. Hybrid sensor fusion architectures combining hardware signals with model-based estimates via complementary filtering exploit their complementary frequency-domain characteristics, showing measurable improvements over either approach in isolation [8].

III. HAPTIC FEEDBACK MODALITIES AND HUMAN–MACHINE INTERACTION

Haptic feedback encompasses two mechanistically distinct channels. Kinesthetic feedback stimulates tendon, joint, and deep muscle receptors via forces applied to the operator's limbs, conveying force magnitude and direction. Cutaneous/tactile feedback stimulates skin mechanoreceptors via surface deformations or vibrations, conveying texture, edge detection, and slip-onset cues [18]. The most naturalistic haptic experience combines both channels, though implementation constraints often necessitate a choice between them. Fig. 2 summarizes the resulting taxonomy of modalities surveyed in this section.

A. Kinesthetic Force Reflection

Kinesthetic feedback drives master-side actuators in opposition to slave-measured forces, with performance governed by the transparency criterion of the teleoperation two-port hybrid matrix [6]. A perfectly transparent system yields $H = \left[\begin{smallmatrix} 0 & 1 \\ -1 & 0 \end{smallmatrix}\right]$, faithfully transmitting slave environment impedance to the operator. In practice, backdrivability limits, friction, and sensor noise constrain achievable transparency. The Sigma.7 interface (Force Dimension) provides six-degree-of-freedom (6-DOF) force output with 20 N continuous and >40 N peak per axis [19]. Stability under time delay is the critical safety constraint. Even local teleoperation accumulates 10–30 ms latency. Wave variable transformation [7] guarantees stability for arbitrary constant delays; Time-Domain Passivity Control (TDPC) [20] provides improved performance for variable delays by inserting dissipation precisely when energy passivity violations are detected.

B. Vibrotactile Feedback

Vibrotactile transducers stimulate Meissner and Pacinian corpuscle mechanoreceptors, with Pacinian receptors exhibiting peak sensitivity at 250–300 Hz. Linear resonant actuators (LRAs) provide flat frequency response and repeatability; piezoelectric bimorphs enable precise waveform control across 1 Hz–5 kHz. Amplitude modulation reliably encodes grasping force magnitude, while high-frequency onset transients signal slip-onset—detectable tens of milliseconds before visible tissue deformation [10]. Talasaz et al. [22] demonstrated that vibrotactile slip feedback reduced slip events by 32% versus visual feedback alone in bench-top trials. The primary advantage over kinesthetic feedback is implementability: vibration actuators integrate into console handles without backdrivability or stability constraints. The da Vinci 5 includes vibrotactile feedback through instrument grips alongside its kinesthetic channel [2].

C. Pneumatic and Electrotactile Feedback

Pneumatic tactile displays employ arrays of 4×4 to 8×8 independently addressable micro-actuators on fingertip thimbles, with cell pitches of 2–4 mm matching slowly-adapting type I (SAI) receptor spatial resolution thresholds. Advantages include inherent safety, magnetic resonance (MR) compatibility, and rich spatial information [23]. Switching latency of 20–80 ms is a practical concern. Electrotactile stimulation directly activates cutaneous mechanoreceptors via controlled current pulses, achieving microsecond hardware latency with compact electrode geometries, but faces regulatory and comfort barriers for surgical application [24].

D. Sensory Substitution

Visual force overlays using color-coded augmented reality (AR) annotations have demonstrated modest benefits in laboratory settings, with utility during live surgery limited by attentional competition with the operative field. Auditory feedback encoding force magnitude or slip onset shows promise as a cognitive-load-appropriate complement [25]. Kitagawa et al. [25] demonstrated that auditory sensory substitution significantly affected suture manipulation forces in robotic surgical systems.

TABLE II
HAPTIC FEEDBACK MODALITY COMPARISON

Modality	Freq.	Lat. (ms)	Fidelity	Impl.	Key Ref.
Kinesthetic	DC–50 Hz	5–30	High	Complex	[19], [20]
Vibrotactile (LRA)	40–300 Hz	2–10	Moderate	High	[22]
Vibrotactile (PZT)	1 Hz–5 kHz	<2	High	Moderate	[21]
Pneumatic Array	0–20 Hz	20–80	Moderate	Moderate	[23]
Electrotactile	DC–1 kHz	<1	Moderate	Challenging	[24]
Visual (AR)	N/A	Frame	Low–Mod.	Very High	—

Sources: [10], [19]–[24]

IV. AI-BASED INTERACTION FORCE ESTIMATION

AI-based force estimation exploits sensor modalities already present in surgical robots—endoscopic video, joint encoders, and motor current—to infer contact forces without additional hardware. The central premise is that soft tissue deformation under contact forces produces observable visual signatures decodable with sub-Newton accuracy [11], [12].

A. Vision-Based Deep Learning

Chua et al. [11] demonstrated real-time force estimation from camera images and robot state on a da Vinci Research Kit. Their single-frame network fused ResNet-50 image features with the robot-state vector to regress three-axis force, reaching a mean RMSE near 0.31 N across all axes on silicone artificial tissue while running at video rate. Combining image and state inputs gave the best mean accuracy across viewpoints and workspace positions, outperforming the vision-only variant and a physics-based baseline. Masui et al. [26] applied a VGG-16 convolutional network to endoscopic images of excised porcine kidney, reporting a normalized RMSE of 8.7% and showing that restricting the analyzed image region to the forceps tips was decisive for accuracy. Transformer architectures with self-attention mechanisms capture long-range temporal dependencies in viscoelastic tissue deformation dynamics, reducing errors during transient loading phases [12], [27].

B. Physics-Informed Neural Networks

Physics-informed neural networks (PINNs) embed tissue biomechanics knowledge directly into training by augmenting data-fitting loss with physics-based residual terms:

$$\mathcal{L}_{\text{total}} = \mathcal{L}_{\text{data}} + \lambda_{\text{phys}}\,\mathcal{L}_{\text{physics}} + \lambda_{\text{BC}}\,\mathcal{L}_{\text{BC}} \tag{3}$$

where $\mathcal{L}_{\text{physics}}$ penalizes violations of continuum mechanics equilibrium equations at collocation points within the tissue domain, and $\mathcal{L}_{\text{BC}}$ enforces boundary conditions [28].

C. Reinforcement Learning and Adaptive Estimation

Reinforcement learning (RL) frameworks treat surgical manipulation as a Markov decision process with force- and safety-aware reward shaping. Pore et al. [29] developed a safe deep-RL framework for autonomous tissue retraction that embeds safety constraints during training and applies formal verification to bound the probability of unsafe configurations, keeping the instruments within a safe operating workspace. Gaussian process regression (GPR) provides principled online adaptive tissue model updating during procedures, representing tissue response as a Gaussian process and updating the posterior as force-deformation observations accumulate. The inherent uncertainty quantification can flag poorly characterized tissue regions, triggering additional tactile exploration before critical manipulation steps [30].

D. Real-Time Deployment Constraints

Human haptic temporal resolution for force direction changes is approximately 5–10 ms; feedback loop closure at $\geq$30 Hz is necessary to prevent perceptible temporal distortion [31]. Embedded graphics processing unit (GPU) inference on NVIDIA Jetson Xavier/Orin platforms achieves ResNet-50 throughput of 60–120 FPS for single images, sufficient for video-rate force feedback [32]. However, streaming inference on high-resolution endoscopic video concurrent with robot control, safety monitoring, and AR rendering demands careful real-time scheduling and hardware partitioning. Validation datasets remain predominantly phantom- and ex-vivo-based; generalization to in vivo human tissue remains an open challenge [12].

V. KEY CHALLENGES

A. Miniaturization and Sterilization

The most fundamental hardware constraint is co-optimizing sensing element miniaturization within 5–12 mm trocar-compatible dimensions while maintaining clinical accuracy, drift, and durability. FBG sensors represent the current state of the art but require sterilization-compatible optical connectors at the sterile field boundary. High-vacuum steam sterilization at 134°C causes thermal expansion mismatches, adhesive delamination, and moisture ingress through microcracks. Hermetic packaging at millimeter scales using laser-welded titanium or ceramic feedthroughs is feasible but incurs fabrication costs incompatible with commercial disposable instrument models.

B. Latency and Real-Time Architecture

Haptic feedback is acutely latency-sensitive. The human haptic system detects force perturbations within 2–5 ms and shows perceptible transparency degradation when loop delays exceed 15–30 ms [33]. AI-based estimation adds 5–20 ms for optimized embedded GPU implementations, consuming a significant fraction of the available budget. Real-time operating systems and field-programmable gate array (FPGA)-based signal processing reduce scheduling jitter to below 100 μs. FPGA-integrated AI inference, while feasible via high-level synthesis, limits post-deployment architecture updates—a concern for artificial intelligence/machine learning (AI/ML)-based Software as a Medical Device (SaMD) under FDA guidelines requiring re-evaluation of algorithm updates [34].

C. Regulatory and Validation Barriers

Medical devices incorporating software-driven force feedback must navigate evolving regulatory pathways. The FDA SaMD framework and AI/ML SaMD guidelines introduce requirements for algorithm transparency, validation across clinically representative populations, and post-market performance monitoring [34], [35]. The European Union Medical Device Regulation (EU MDR) 2017/745 imposes analogous requirements. Clinical validation methodology remains unsettled: most published evidence derives from laboratory task metrics rather than clinical outcome measures—complication rates, anastomotic integrity—demanding large multicenter prospective studies [4], [36].

D. Economic Barriers in LMIC Contexts

Capital costs of currently deployed robotic platforms ($1.5–2.5 million USD for da Vinci Xi, plus $100,000–$200,000 annual service) restrict adoption to tertiary hospitals in high-income countries and a small number of high-resource facilities in middle-income nations [37]. In the Nigerian context, as of 2024, robotic surgical installations remain concentrated in fewer than five centers nationally, with maintenance infrastructure and technical support underdeveloped relative to peer nations [44], [45]. Total ownership costs must further account for per-use instrument costs ($700–$3,500 per case), calibration requirements in environments with humidity, temperature, and power quality fluctuations, and biomedical engineering workforce development.

VI. Proposed Conceptual Framework for Next-Generation Force-Aware Surgical Robots

The foregoing analysis motivates a three-layer co-designed framework integrating force sensing, AI estimation, and haptic feedback as a unified architecture rather than separately developed subsystems. The framework is organized around: (1) a Perception Layer for force and state sensing; (2) an Estimation and Intelligence Layer for sensor fusion, model-based estimation, and AI inference; and (3) a Feedback and Control Layer closing the loop to the surgeon's haptic interface with safety supervision. Fig. 3 illustrates the resulting closed-loop architecture.

A. Perception Layer

The Perception Layer deploys a heterogeneous sensing strategy: FBG sensors embedded in the distal 30 mm of the instrument shaft for direct force measurement, joint torque estimation from motor current across all actuated joints for full-robot contact detection, and stereoscopic 4K endoscopic video for visual force estimation. FBG sensors are selected for electromagnetic immunity, biocompatibility, and demonstrated sterilization durability. The 30 mm distal span is a design assumption, not an optimized value: it approximates the rigid segment between tool tip and wrist articulation on typical laparoscopic instruments, keeping the gratings clear of the high-flexion joint identified earlier as a fragility point. A specific instrument geometry would refine this figure. A multi-rate acquisition architecture is proposed: FBG interrogation at 1 kHz for tissue texture and slip detection, joint-level torque estimation synchronous with the 1 kHz control loop, and 60 Hz endoscopic frames passed asynchronously to the Estimation Layer with inter-frame force interpolation. Interrogating the FBGs at 1 kHz matches the servo control rate, so that optical force samples and joint-torque estimates share a single timebase and fuse without resampling—the synchronization the fusion stage depends on. The 1 kHz figure follows typical surgical-manipulator servo rates rather than a rate optimized for FBG-based tissue discrimination, and would need confirming against the selected interrogator hardware.

B. Estimation and Intelligence Layer

A hierarchical parallel inference architecture combines multiple pathways fused by inverse-variance weighting. The primary pathway fuses FBG signals and joint torques via an Unscented Kalman Filter (UKF) parameterized by patient-specific constitutive parameters identified during an initial exploratory palpation phase. The duration, protocol, and tissue coverage of this phase remain unspecified and would need empirical tuning to balance identification accuracy against added procedure time. The secondary pathway applies a PINN-based visual force estimator to produce an independent six-axis wrench estimate with prediction uncertainty. The fusion module naturally downweights the visual estimate during tool occlusion or image degradation from blood, smoke, or irrigation fluid. An online GPR module continuously updates tissue constitutive parameters during the procedure, adapting to intraoperative property changes from electrosurgery thermal effects and tissue preconditioning.

C. Numerical Validation of the Fusion Mechanism

The claim that inverse-variance fusion downweights a degraded channel is tested here with a synthetic Monte Carlo simulation rather than left as an unverified assertion. A ground-truth grasp-hold-release force profile (0–5 N over 3 s, sampled at the 1 kHz primary loop rate) is corrupted with independent Gaussian noise on two channels: an FBG-like channel at its nominal Table I resolution (0.08 N) and a joint-torque-like channel at its nominal model-based resolution (0.30 N). A 0.6 s window (t = 1.2–1.8 s) simulates the fiber fragility at articulated wrist joints noted in Section II-C by spiking the FBG noise to 1.2 N while the joint-torque channel is unaffected; the two channels are combined by the inverse-variance weighting described above. Fig. 4 shows a representative trial and the resulting RMSE over 200 Monte Carlo trials. The fused estimate achieves 0.147 N RMSE overall, a 72.9% reduction relative to the FBG-only channel (0.543 N) and 50.9% relative to the joint-torque-only channel (0.300 N). During the simulated degradation window, FBG-only RMSE rises to 1.204 N while the fused estimate remains at 0.291 N—within 3% of the joint-torque-only channel (0.300 N)—indicating that the fusion falls back toward the better-behaved sensor rather than inheriting the degraded channel's error.

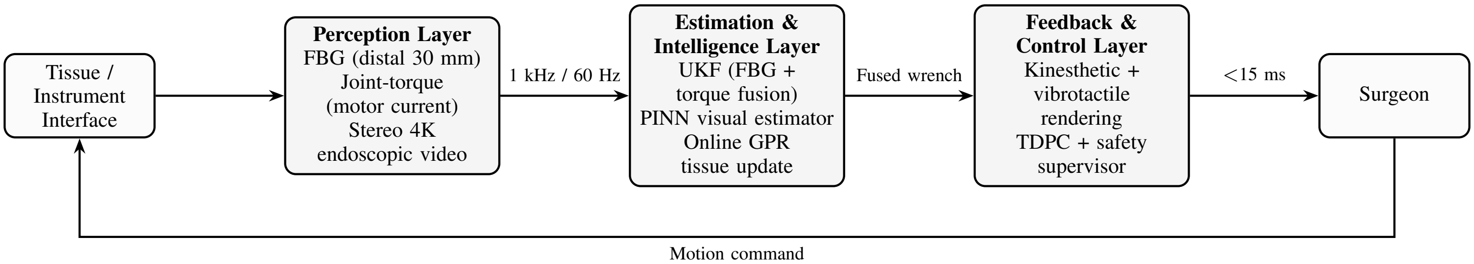

Fig. 3. Closed-loop, three-layer architecture of the proposed force-aware framework. Sensing (Perception Layer) feeds a hierarchical fusion pipeline (Estimation and Intelligence Layer), which drives multimodal haptic rendering with safety supervision (Feedback and Control Layer) back to the surgeon, whose motion commands re-enter the loop at the instrument-tissue interface.

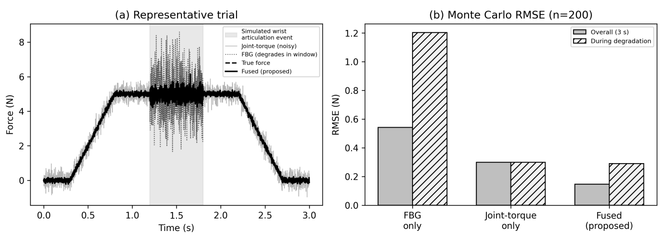

Fig. 4. Monte Carlo simulation (200 trials) of inverse-variance fusion between a synthetic FBG-like channel and a synthetic joint-torque-like channel. (a) A representative trial, with the shaded region marking a simulated wrist-articulation event during which FBG noise is increased. (b) RMSE of each channel and the fused estimate, computed over the full trial and restricted to the degradation window.

This result validates the fusion *logic* under stated conditions, not a hardware outcome: the ground-truth profile and noise levels are synthetic, drawn from the Table I resolution ranges rather than measured; the fusion weights use the true instantaneous noise variance, an idealization of what an online UKF would need to estimate from its own covariance propagation; the two channels' noise is assumed independent; and only one degradation mode is tested, out of the several named in Sections V and VI-B. Full detail on these conditions is consolidated in the Limitations (Section VII-A) rather than repeated here.

D. Feedback and Control Layer

The Feedback and Control Layer renders estimated force vectors via a multimodal haptic interface combining kinesthetic force reflection at the hand controllers with vibrotactile stimulation at fingertip interfaces. A variable impedance controller reduces scaling gains during tissue approach (where sensitivity is paramount) and increases them during active manipulation (where force magnitude safety is critical). Time-Domain Passivity Control (TDPC) [20] monitors haptic channel energy passivity in real time, inserting dissipation to prevent instability from estimation noise or communication jitter. A safety supervisory module monitors estimated contact forces against tissue-specific injury thresholds from the biomechanics literature, issuing an early warning once the estimated force reaches 60% of the applicable injury threshold. The 60% figure is a conservative early-warning margin rather than an established clinical value: it leaves headroom below the damage limit for force-estimation error and surgeon reaction time, and the exact fraction would be calibrated per tissue type during clinical validation. When estimated forces cross this margin, a distinctive vibrotactile warning pattern and AR overlay are triggered; approaching the full threshold activates a virtual fixture constraint that imposes increasing haptic resistance while allowing surgeon override when clinically necessary. The end-to-end latency target for the complete feedback loop is <15 ms. This figure follows from the perceptual limits noted earlier: the haptic system resolves force perturbations on a 2–5 ms scale and transparency begins to degrade once loop delay passes 15–30 ms, so holding the full loop under 15 ms keeps it below the onset of perceptible degradation.

To assess the feasibility of this target, Table III decomposes the projected pipeline latency into per-stage contributions. These figures are an analytical projection based on representative values reported for comparable embedded implementations in the surveyed literature, not measured results from a built system; actual performance will depend on the specific interrogator, compute platform, and actuator hardware selected. The PINN-based visual pathway is excluded from the critical-path sum because it runs asynchronously at the 60 Hz frame rate and is merged into the fused estimate via inter-frame interpolation rather than gating the 1 kHz primary loop; when active, it contributes an additional 8–17 ms per frame on embedded GPU platforms [32], which the fusion module accommodates through its own update cycle rather than by stalling the haptic loop.

The projected total leaves a margin of roughly 10 ms against the 15 ms target, which is intended to absorb estimation-error correction, scheduling jitter, and surgeon reaction time rather than to be consumed by the sensing and rendering pipeline itself. This margin is consistent with the 60% early-warning threshold in the safety supervisory module: both are conservative allowances against the same class of unmodeled delay and error, not independently derived figures.

VII. Clinical Implications and Future Research Directions

The meta-analytic evidence from Bergholz et al. [4] indicates standardized mean differences of 0.83 (95% CI 0.63–1.03) and 0.69 (95% CI 0.51–0.87) for average and peak force

TABLE III
PROJECTED END-TO-END LATENCY BUDGET OF THE PRIMARY (FBG + UKF) PATHWAY

Pipeline Stage	Est. (ms)	Basis
FBG interrogation (1 kHz sample period)	1.0	Sec. VI-A design rate
Joint-torque sampling (motor current)	0.2	Synchronous, 1 kHz loop
UKF sensor fusion (low-dim. state)	1.0	Embedded observer rate [17]
TDPC computation + haptic command generation	0.5	Real-time control loop [20]
Kinesthetic actuator response	1.5	Force-feedback device class [19]
Local sensor–controller–actuator bus overhead	1.0	Wired bedside architecture
Projected total (critical path)	**≈5.2**	
Margin to 15 ms target	**≈9.8**	

TABLE IV
COMPARISON OF COMMERCIAL PLATFORMS VS. PROPOSED FRAMEWORK

System	Force Sensing	Haptic Feedback	AI Est.	Key Limitation
da Vinci Xi [1]	None at tip	None	None	Visual-only feedback
da Vinci 5 [2], [5]	Push-pull tip	Kines. + vibro.	Limited	1-axis; high cost
Versius [38]	Collision detect. (binary)	Discrete audio + visual alarm	None	No continuous F/T sensing
Senhance [40]	Marketed	Tactile	Limited	Validation gap
Hugo RAS [39]	Joint torques	None	None	Emerging platform
Proposed	FBG 6-axis + joint	Kines. + vibro. + AR	PINN + UKF + GPR	Conceptual*

*Projected latency (Table III) and fusion accuracy (Fig. 4) are analyzed quantitatively in Section VI; other rows reflect qualitative platform capabilities as reported in the cited sources.

reductions with haptic versus no-haptic feedback. For suturing and anastomotic tasks, excess needle driver forces plausibly contribute to anastomotic ischemia by compressing mucosal blood flow—a hypothesis warranting prospective multicenter investigation [41]. Haptic force metrics also offer objective trainee performance assessment unavailable on standard platforms.

For the Nigerian context, the AI-only pathway—using exclusively cameras and joint encoders already present on deployed platforms—offers a near-zero additional hardware cost route to improved force estimation compatible with software updates to existing systems. The computational infrastructure required (NVIDIA Jetson Orin equivalent: \$500–\$2,000) is suitable for integration into new platform development without specialized semiconductor supply chains.

Priority future research directions include: (1) in vivo ground-truth force datasets via instrumented trocar systems and miniature implantable reference sensors, addressing the critical phantom-to-clinical generalization gap [12]; (2) flexible electronics sensor arrays on elastomeric substrates for distributed pressure mapping; (3) federated learning for multi-institutional AI model training without centralizing raw patient data [42]; (4) foundation model adaptation of large pre-trained multimodal architectures to surgical scenes [43]; and (5) LMIC-adapted robotic platform development.

A. Limitations

The proposed framework is conceptual, not built or clinically validated, and several specifics—the 30 mm FBG placement, 1 kHz interrogation rate, 60% early-warning margin, and <15 ms latency target—are design assumptions, not measured or optimized values, to be refined once a specific instrument geometry, interrogator, and control platform are selected. The latency budget in Table III is similarly an analytical projection from literature-representative figures, not a measurement, and excludes network-induced jitter should any component be deployed non-locally. The evidentiary base for haptic and AI-based force estimation benefits (Section VII) is drawn predominantly from phantom, ex-vivo, and high-income-country settings; none of the cited studies were conducted on African patients or within Nigerian clinical infrastructure, so the deployment-feasibility claims here remain to be tested empirically, not assumed to transfer directly. This review includes no original hardware or in-vivo results; the Monte Carlo fusion simulation (Section VI-C) validates one sub-component's logic under synthetic conditions and is not evidence for the full closed-loop system's performance. The paper's central contribution remains the synthesis, gap analysis, and conceptual integration above, addressed by the priority research directions in this section.

VIII. CONCLUSION

This paper has presented a comprehensive review of force sensing technologies, haptic feedback modalities, and AI-based force estimation for robot-assisted minimally invasive surgery, culminating in a three-layer conceptual framework for next-generation force-aware surgical robots. The central argument is that clinical progress in restoring haptic perception requires treating these three domains as a unified co-designed system, leveraging complementary strengths to compensate for individual limitations that have prevented any single approach from achieving comprehensive clinical translation.

FBG-based optical sensing has reached a maturity supporting clinical translation for distal instrument sensing, pending resolution of interrogator cost and optical connector durability. AI-based estimation provides a complementary pathway supplementing hardware sensing during occlusion and offering cost-effective primary sensing for platforms where hardware integration is infeasible. Haptic feedback—both kinesthetic and vibrotactile—demonstrates robust experimental evidence of force reduction and performance improvement, with meta-analytic evidence now sufficiently mature to support regulatory submissions. A Monte Carlo simulation further indicates that inverse-variance fusion of FBG and joint-torque estimates degrades gracefully rather than failing outright when one channel is impaired—evidence the fusion logic, though not yet hardware-validated, is soundly specified.

The most pressing near-term priorities are in vivo validated force datasets, demonstration of clinical outcome benefits beyond task performance metrics, and economically viable manufacturing approaches for force-sensing instruments. For the Nigerian and broader West African context, investment in technical training infrastructure, AI estimation model validation on African patient populations, and engagement with regulatory frameworks represent the most actionable near-term steps toward making force-aware robotic surgery available globally.

Acknowledgment

The authors acknowledge the Department of Electronic and Electrical Engineering, Obafemi Awolowo University, Ile-Ife, Nigeria, for institutional support.

References

[1] Intuitive Surgical, Inc., "da Vinci surgical systems: Product overview and clinical applications," Intuitive Surgical Annual Report, 2023.

[2] Intuitive Surgical, Inc., "da Vinci 5 technical specifications and Force Feedback technology," Intuitive Surgical White Paper, 2024.

[3] J. Rosen et al., "Biomechanical properties of abdominal organs in vivo and postmortem under compression loads," *J. Biomech. Eng.*, vol. 130, no. 2, art. 021020, 2008.

[4] M. Bergholz et al., "The benefits of haptic feedback in robot assisted surgery: A systematic review and meta-analysis," *Sci. Rep.*, vol. 13, p. 19215, 2023.

[5] M. M. Awad et al., "Evaluation of forces applied to tissues during robotic-assisted surgical tasks using a novel force feedback technology," *Surg. Endosc.*, vol. 38, no. 10, pp. 6193–6202, 2024.

[6] D. A. Lawrence, "Stability and transparency in bilateral teleoperation," *IEEE Trans. Robot. Autom.*, vol. 9, no. 5, pp. 624–637, 1993.

[7] G. Niemeyer and J.-J. E. Slotine, "Stable adaptive teleoperation," *IEEE J. Ocean. Eng.*, vol. 16, no. 1, pp. 152–162, 1991.

[8] A. H. H. Hosseinabadi et al., "Force sensing in robot-assisted keyhole endoscopy: A systematic survey," *Int. J. Rob. Res.*, vol. 41, no. 2, pp. 136–162, 2022.

[9] Y. Hao et al., "Development of force sensing techniques for robot-assisted laparoscopic surgery: A review," *IEEE Trans. Med. Robot. Bionics*, vol. 6, no. 3, pp. 868–887, 2024.

[10] I. Sarakoglou et al., "A high performance tactile feedback display and its integration in teleoperation," *IEEE Trans. Haptics*, vol. 5, no. 3, pp. 252–263, 2012.

[11] Z. Chua et al., "Toward force estimation in robot-assisted surgery using deep learning with vision and robot state," in *Proc. ICRA*, 2021, pp. 12335–12341.

[12] M. Pan, "A review of image-based sensorless force estimation in robotic-assisted medical interventions," *Neurocomputing*, vol. 605, p. 128372, 2026.

[13] P. Puangmali et al., "Miniature 3-axis distal force sensor for minimally invasive surgical palpation," *IEEE/ASME Trans. Mechatron.*, vol. 17, no. 4, pp. 646–656, 2012.

[14] M. I. Tiwana et al., "A review of tactile sensing technologies with applications in biomedical engineering," *Sens. Actuators A*, vol. 179, pp. 17–31, 2012.

[15] S. Dong et al., "Fiber Bragg grating force sensors for minimally invasive surgery: State of the art, challenges, and opportunities," *SmartBot*, vol. 2, no. 1, e2400015, 2025.

[16] FBGS International, "FBG Principle," 2024. [Online]. Available: https://fbgs.com/technology/fbg-principle/

[17] A. De Luca et al., "Collision detection and safe reaction with the DLR-III lightweight manipulator arm," in *Proc. IROS*, 2006, pp. 1623–1630.

[18] R. S. Johansson and J. R. Flanagan, "Coding and use of tactile signals from the fingertips in object manipulation tasks," *Nat. Rev. Neurosci.*, vol. 10, no. 5, pp. 345–359, 2009.

[19] Force Dimension, "Sigma.7 force-feedback device specifications," Force Dimension Tech. Dec., 2024.

[20] J. H. Ryu et al., "Stable teleoperation with time domain passivity control," *IEEE Trans. Robot. Autom.*, vol. 20, no. 2, pp. 365–373, 2004.

[21] H. Culbertson et al., "Haptics: The present and future of artificial touch sensation," *Annu. Rev. Control Robot. Auton. Syst.*, vol. 1, pp. 385–409, 2018.

[22] A. Talasaz et al., "The role of direct and visual force feedback in suturing using a 7-DOF dual-arm teleoperated system," *IEEE Trans. Haptics*, vol. 10, no. 2, pp. 276–287, 2017.

[23] C. Pacchierotti et al., "Wearable haptic systems for the fingertip and the hand: Taxonomy, review, and perspectives," *IEEE Trans. Haptics*, vol. 10, no. 4, pp. 580–600, 2017.

[24] S. S. Srinivasan et al., "On prosthetic control: A regenerative agonist-antagonist myoneural interface," *Sci. Robot.*, vol. 2, no. 6, eaan2971, 2017.

[25] M. Kitagawa et al., "Effect of sensory substitution on suture-manipulation forces for robotic surgical systems," *J. Thorac. Cardiovasc. Surg.*, vol. 129, no. 1, pp. 151–158, 2005.

[26] K. Masui et al., "Vision-based estimation of manipulation forces by deep learning of laparoscopic surgical images obtained in a porcine excised kidney experiment," *Sci. Rep.*, vol. 14, p. 9686, 2024.

[27] S. Wang et al., "Linformer: Self-attention with linear complexity," arXiv:2006.04768, 2020.

[28] M. Raissi et al., "Physics-informed neural networks," *J. Comput. Phys.*, vol. 378, pp. 686–707, 2019.

[29] A. Pore et al., "Safe reinforcement learning using formal verification for tissue retraction in autonomous robotic-assisted surgery," in *Proc. IEEE/RSJ IROS*, 2021, pp. 4025–4031.

[30] Y. Li and B. Hannaford, "Gaussian process regression for sensorless grip force estimation of cable-driven elongated surgical instruments," *IEEE Robot. Autom. Lett.*, vol. 2, no. 3, pp. 1312–1319, 2017.

[31] R. T. Verrillo, "Psychophysics of vibrotactile stimulation," *J. Acoust. Soc. Am.*, vol. 77, no. 1, pp. 225–232, 1985.

[32] D. Pisla et al., "An AI-based sensorless force feedback method in robot-assisted minimally invasive surgery," *Information*, vol. 16, no. 11, p. 993, 2025.

[33] R. J. Adams and B. Hannaford, "Stable haptic interaction with virtual environments," *IEEE Trans. Robot. Autom.*, vol. 15, no. 3, pp. 465–474, 1999.

[34] FDA CDRH, "AI/ML-based software as a medical device action plan," FDA, 2021.

[35] J. He et al., "The practical implementation of artificial intelligence technologies in medicine," *Nat. Med.*, vol. 25, no. 1, pp. 30–36, 2019.

[36] E. L. Servais et al., "Novel force feedback technology improves suturing in robotic-assisted surgery: A pre-clinical study," *Surg. Endosc.*, vol. 39, no. 2, pp. 1217–1226, 2025.

[37] K. H. Sheetz et al., "Trends in the adoption of robotic surgery for common surgical procedures," *JAMA Netw. Open*, vol. 3, no. 1, e1918911, 2020.

[38] CMR Surgical Ltd, "Versius Surgical System User Manual," Version 15.0, Doc. No. U-00009v15.0, Cambridge, UK, Feb. 2021.

[39] J. C. Ngu, C. C. Lin, C. J. Sia, and N. Teo, "A narrative review of the Medtronic Hugo RAS and technical comparison with the Intuitive da Vinci robotic surgical system," *J. Robotic Surg.*, vol. 18, no. 1, art. 99, 2024.

[40] R. V. Patel, S. F. Atashzar, and M. Tavakoli, "Haptic feedback and force-based teleoperation in surgical robotics," *Proc. IEEE*, vol. 110, no. 7, pp. 1012–1027, Jul. 2022.

[41] J. C. Slieker et al., "Systematic review of the technique of colorectal anastomosis," *JAMA Surg.*, vol. 148, no. 2, pp. 190–201, 2013.

[42] N. Rieke et al., "The future of digital health with federated learning," *NPJ Digit. Med.*, vol. 3, p. 119, 2020.

[43] M. Moor et al., "Foundation models for generalist medical artificial intelligence," *Nature*, vol. 616, no. 7956, pp. 259–265, 2023.

[44] A. F. Falola, S. Singh, U. Das, A. Oluwagbemi, R. Etta, and A. Adeyeye, "Barriers and recommendations for the implementation of robot-assisted minimally invasive surgery in Africa," *J. Robotic Surg.*, vol. 19, no. 1, art. 16, 2024.

[45] V. C. Okebalama et al., "Robotic Surgery in Africa: History, Contemporary, and Thereafter," *Niger. Med. J.*, vol. 66, no. 3, pp. 867–872, 2024.

[46] F. A. Gemechu et al., "Bridging the gap: feasibility and future directions of robotic surgery in Sub-Saharan Africa—a narrative review," *J. Robotic Surg.*, vol. 19, art. 372, 2025.

[47] M. Chepkoech, B. Malila, and J. Mwangama, "Telementoring for surgical training in low-resource settings: a systematic review of current systems and the emerging role of 5G, AI, and XR," *J. Robotic Surg.*, vol. 19, no. 1, art. 525, 2025.